

Lawrence Berkeley National Laboratory

Lawrence Berkeley National Laboratory

Title

RF-driven Proton Source with a Back-streaming Electron Dump

Permalink

<https://escholarship.org/uc/item/7j56m8fk>

Author

Ji, Q.

Publication Date

2009-12-20

Peer reviewed

RF-driven Proton Source with a Back-streaming Electron Dump^{a)}

Q. Ji,^{1,b)} A. Sy,^{1,2} and J. W. Kwan¹

¹Lawrence Berkeley National Laboratory, 1 Cyclotron Road, MS 5R0121, Berkeley, CA 94720, U. S. A.

²Department of Nuclear Engineering, University of California, Berkeley, CA 94720, U. S. A.

This article describes an RF ion source with a back-streaming electron dump. A quartz tube, brazed to a metal plug at one end, is fused in the center of a flat quartz plate. RF power (at 13.6 MHz) is coupled to generate hydrogen plasma using a planar external antenna bonded to the window. Bonding the water-cooled rf antenna to the quartz window significantly lowers its temperature. The water-cooled metal plug serves as the back-streaming electron dump. At 1800W, the current density of extracted hydrogen ions reaches approximately 125 mA/cm².

I. INTRODUCTION

Different antenna configurations have been used in RF-driven ion sources: internal antenna,¹ external helicon antenna,^{2,3} and external planar antenna.⁴ Lifetime has always been an issue for internal antenna. Ion sources with external planar antenna produce high-density plasma and exhibit long lifetime, but the dielectric window used as the back plate in the ion source is vulnerable to back-streaming electron bombardment. An ion source with an innovative RF window design has been built at Lawrence Berkeley National Laboratory. A quartz tube, brazed to a metal plug at one end, is fused in the center of the RF window. The water-cooled metal plug serves as the back-streaming electron dump.

II. RF-DRIVEN ION SOURCE WITH A BACK-STREAMING ELECTRON DUMP

A. Ion source design

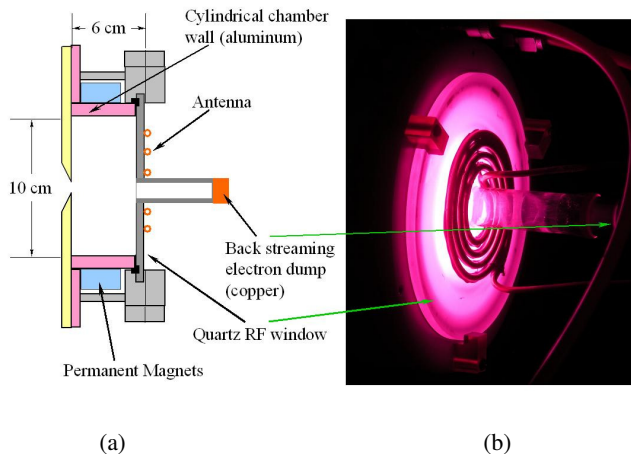


FIG. 1. (a). Schematic drawing of the RF ion source with a back-streaming electron dump. (b) A photograph of the ion source in operation.

A schematic drawing of the source is shown in Figure 1(a). The ion source has a 10-cm ID, 6-cm-tall chamber with an air-

cooled quartz window at the back. RF power (at 13.6 MHz) is coupled to the plasma using a planar external antenna at the window. Water-cooled permanent magnets are embedded in the cylindrical wall to create the “multicusp” magnetic configuration for improved plasma confinement. The wall material is aluminum. The quartz window is o-ring sealed directly to the chamber wall. A quartz tube, brazed to a metal plug at one end, is fused in the center of the RF window. The water-cooled metal plug serves as the back-streaming electron dump. As seen from the photograph of the source in operation in Fig. 1 (b), plasma was localized in the main source chamber. Minimal plasma diffused to the quartz tube with electron dump.

B. Optimization of RF antenna

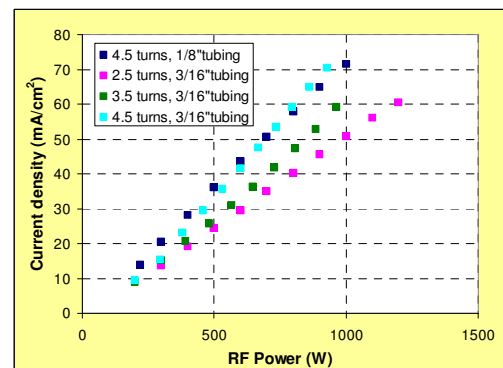


FIG. 2. Comparisons of the extracted ion beam current density from ion sources with various type of RF antenna.

Copper tubing has been used as RF antenna to couple RF signal into the plasma chamber. Different sizes of copper tubing with various turns have been compared. Fig. 2 shows the extracted ion beam current density from the source with 1/8”-diameter and 3/16”-diameter copper tubings. The number of turns varied from two and a half to four and a half. With the same size tubing, the ion source with an antenna of higher number of turns produced larger current density. Four and a half turns, 3/16”-diameter copper antenna offered the best RF signal coupling to the plasma. The performances of 1/8” and 3/16” tubing for the same antenna configuration of four and a half turns are similar. The 3/16” tubing, however, exhibited several disadvantages:

a) Contributed, published as part of the Proceedings of the 13th International Conference on Ion Sources, Gatlinburg, Tennessee, September, 2009.

b) qji@lbl.gov

thicker tubing is harder to bend during antenna fabrication, and the thicker tubing resulted in an antenna whose outermost loop closely approached the source chamber wall. When the source was operated at RF power over 1200W, the plasma was not very stable; this is believed to result from RF coupling into source chamber. Therefore, in the final design, a copper antenna with 4.5 turns, 1/8" tubing was employed.

C. RF window engineering

Good heat dissipation of the RF window, especially in cw operation mode, helps to prolong source lifetime. Simulations using ANSYS were carried out to analyze the heat distribution on the quartz RF window.

1. ANSYS simulation

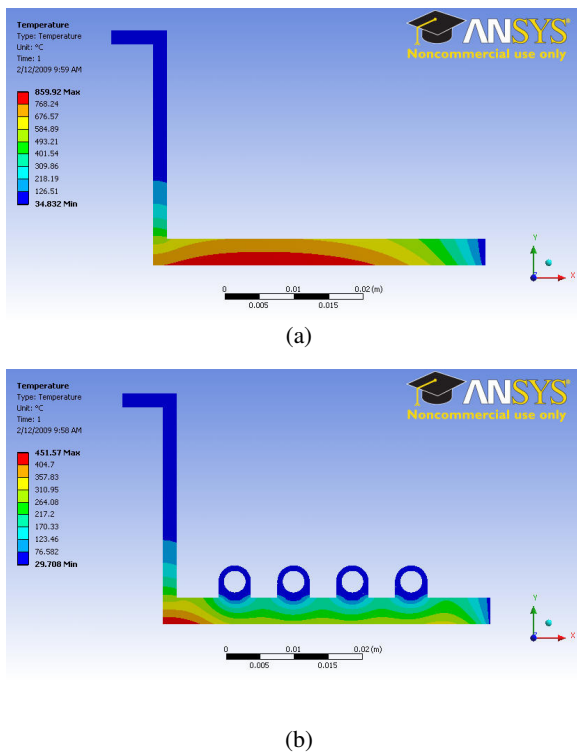


FIG. 3. ANSYS simulation of heat distribution on the quartz rf window: (a) No bonding between the RF antenna and Quartz window; and (b) a water-cooled RF antenna is bonded to the quartz window.

Air- and water-cooling at the beam dump were taken into account. Room temperature was assumed at both the electron dump and the edge of the quartz window. Fig. 3 shows the heat distribution on the quartz RF window when operated at RF power of 2000 W. When the RF antenna is in loose contact with the quartz window, the temperature at the side facing the plasma can reach as high as 850°C, as shown in Fig.3 (a). Bonding the water-cooled RF antenna to the quartz window helps to dissipate heat quickly and more evenly, significantly lowering the window temperature. According to the simulation result in Fig. 3(b), the “hotspot” is located at the center of the rf window, on the side

facing the plasma. At 2000 W, the temperature of the hotspot is reduced to 450°C through bonding of the antenna to the window. The outer surface was kept rather “cool”, with temperatures around 150°C.

2. Measured temperature of Quartz rf window

Temperature of the quartz RF window was measured using ThermoVision™ A20 M infrared camera. Fig. 4(a) illustrates the temperature distribution on the quartz window when the ion source was operated at 2000 W, with the RF antenna bonded to the quartz window. Temperatures of five different spots on the quartz window were monitored when RF operating power was increased. Fig. 4(b) shows the temperature of Spot 1–5 on the quartz window as a function of RF power. Because the maximum measurable temperature of the camera is 350 °C, no data was collected beyond this point; extrapolated temperatures are plotted in Fig. 4(b) as dashed lines.

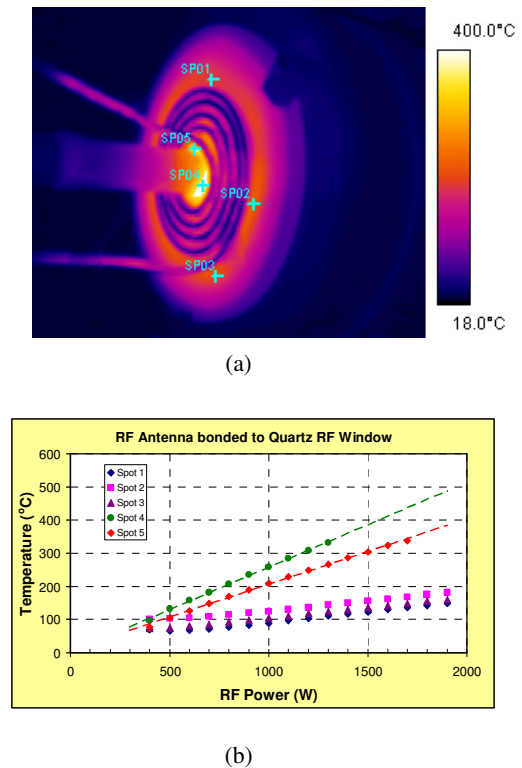


FIG. 4. (a) Temperature of the quartz window measured using a ThermoVision™ A20 M infrared camera. (b) Temperatures of Spot 1-5 on the quartz RF window bonded to the water-cooled RF antenna, as labeled in (a), increase as RF power increases.

The “hotspot” shown in the photograph in Fig. 4(a) is in the center of the quartz, around the joints of quartz plate and tubing where metal electron dump is brazed on. This corresponds to the hotspot location predicted in the ANSYS simulations. The temperature at the “hotspot” reached around 500°C, and temperatures near the outermost loop of the antenna were below 200°C; these results are also consistent with the ANSYS simulations.

III. EXPERIMENTAL RESULTS

A. Atomic ion fraction

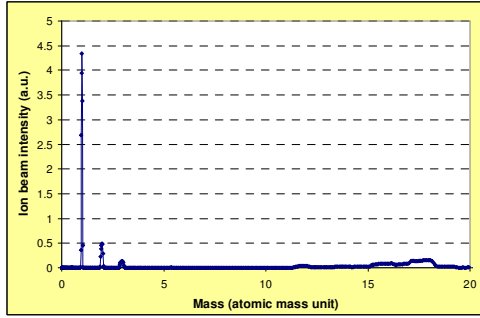


FIG. 5. Mass spectrum of hydrogen plasma generated in the source at RF power of 500 W and source pressure of 9 mTorr.

Hydrogen was used in the experiment. The source was operated at around 9 mTorr. Both atomic H^+ ions and molecular H_2^+ and H_3^+ ions exist in hydrogen plasmas. The mass spectrum of hydrogen plasma generated in this RF-driven ion source has been measured using a magnetic mass spectrometer. Fig. 5 shows the mass spectrum of the plasma at RF power of 500 W and source pressure of 9 mTorr. Over 85% of H^+ has been achieved. As listed in Table I, the atomic ion fraction increases with the RF power, and both H_2^+ and H_3^+ fractions decrease as RF power increases.

TABLE I. Hydrogen ion species fraction vs. RF power.

RF Power (W)	H^+ (%)	H_2^+ (%)	H_3^+ (%)
300	83.0	13.1	3.9
500	87.7	9.7	2.6
1000	91.1	7.9	1.0

B. Extracted current density

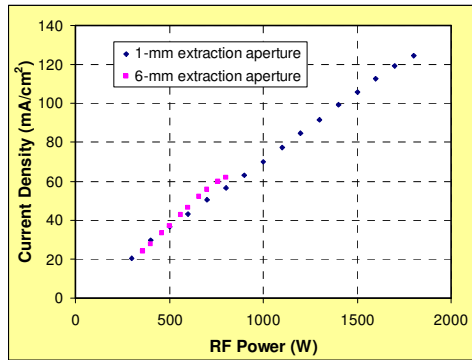


FIG. 6. Extracted ion beam current density as a function of input RF power.

Ion beam were extracted through various aperture size. The measured current density as a function of RF (13.56MHz) power is plotted in Fig. 6, with extraction aperture diameters of 1 mm and 6 mm. The current density extracted from a 6-mm aperture is in agreement with that of a 1-mm aperture, with the 6 mm aperture exhibiting slightly higher extracted beam current density

for RF power above 500 W. At 1800W, the extracted current density reaches approximately 125 mA/cm².

C. Electron current measured on beam dump

A back-streaming electron dump was inserted at the quartz RF window to collect back-streaming electrons when extracting positive ions and to prevent the window from damage. In the experiment, a resistor was connected between the electron dump and plasma electrode to monitor the back-streaming electron current. As shown in Fig. 7, both the extracted proton beam and electron current measured on the beam dump increase as RF power increases, and the back-streaming electron beam follows the same trend as the extracted proton beam. Less than 1 mA of back-streaming electrons was measured when 16 mA of protons were extracted through a 6-mm aperture at RF power of 700 W.

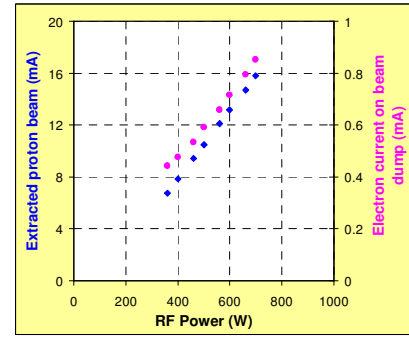


FIG. 7. Both extracted proton beam through a 6-mm aperture and back-streaming electron current monitored on the beam dump increase as RF power increases.

IV. SUMMARY

An RF-driven ion source with a back-streaming electron dump has been fabricated and tested. Bonding water-cooled RF antenna directly to the quartz window significantly lowers the RF window temperature. At 1800W, the extracted hydrogen current density reaches approximately 125 mA/cm². Over 90% of hydrogen ions have been achieved at RF power of 1000W.

V. ACKNOWLEDGEMENTS

The authors would like to thank Jin-Young Jung for his help in ANSYS simulation, and S. B. Wilde, T. McVeigh, and M. Regis for their technical support. This work was supported by IBA Group under Work for Other Agreement Non-Federal Contract No. LB09-005439 and Department of Energy contract No. DE-AC02-05CH11231.

¹Q. Ji, X. Jiang, T.-J. King, K.-N. Leung, K. Standiford, and S. B. Wilde, *J. Vac. Sci. Tech. B*, **20**, 2717(2002).

²X. Jiang, Q. Ji, A. Chang, K.-N. Leung, *Rev. Sci. Instrum.* **74**, 2288 (2003).

³S. K. Hahto, S. T. Hahto, Q. Ji, K.-N. Leung, E. L. Foley, L. R. Grisham, F. M. Levinton, *Rev. Sci. Instrum.* **75**, 355(2004).

⁴J. H. Vainionpaa, T. Kalvas, S. K. Hahto, and J. Reijonen, *Rev. Sci. Instrum.* **78**, 063503(2007).

This document was prepared as an account of work sponsored by the United States Government. While this document is believed to contain correct information, neither the United States Government nor any agency thereof, nor The Regents of the University of California, nor any of their employees, makes any warranty, express or implied, or assumes any legal responsibility for the accuracy, completeness, or usefulness of any information, apparatus, product, or process disclosed, or represents that its use would not infringe privately owned rights. Reference herein to any specific commercial product, process, or service by its trade name, trademark, manufacturer, or otherwise, does not necessarily constitute or imply its endorsement, recommendation, or favoring by the United States Government or any agency thereof, or The Regents of the University of California. The views and opinions of authors expressed herein do not necessarily state or reflect those of the United States Government or any agency thereof or The Regents of the University of California.